

Connectivity Analysis of Wireless Ad Hoc Networks With Beamforming

Xiangyun Zhou, *Student Member, IEEE*, Salman Durrani, *Member, IEEE*, and Haley M. Jones

Abstract—In this paper, we present an analytical model for evaluating the impact of shadowing and beamforming on the connectivity of wireless ad hoc networks accommodating nodes equipped with multiple antennas. We consider two simple beamforming schemes: random beamforming, where each node selects a main beam direction randomly with no coordination with other nodes, and center-directed beamforming, where each node points its main beam toward the geographical center of the network. Taking path loss, shadowing, and beamforming into account, we derive an expression for the effective coverage area of a node, which is used to analyze both the local network connectivity (probability of node isolation) and the overall network connectivity (1-connectivity and path probability). We verify the correctness of our analytical approach by comparing with simulations. Our results show that the presence of shadowing increases the probability of node isolation and reduces the 1-connectivity of the network, although moderate shadowing can improve the path probability between two nodes. Furthermore, we show that the impact of beamforming strongly depends on the level of the channel path loss. In particular, compared with omnidirectional antennas, beamforming improves both the local and the overall connectivity for a path loss exponent of $\alpha < 3$. The analysis in this paper provides an efficient way for system designers to characterize and optimize the connectivity of wireless ad hoc networks with beamforming.

Index Terms—Beamforming, connectivity, effective coverage area, shadowing, wireless ad hoc networks.

I. INTRODUCTION

A WIRELESS ad hoc network consists of self-organizing mobile nodes that can dynamically form a network, with no need for any pre-existing network infrastructure [1]. In such networks, connectivity is a fundamental requirement, i.e., any node pair should be connected either directly or via multiple direct links between intermediate nodes. The study of connectivity of wireless ad hoc networks can broadly be categorized based on whether the individual nodes are equipped with omnidirectional antennas or beamforming antennas. Traditionally, ad hoc networks are assumed to employ omnidirectional antennas, which transmit a signal in all directions with the

Manuscript received November 8, 2008, revised April 15, 2009. First published June 26, 2009; current version published November 11, 2009. This paper was presented in part at the 2008 IEEE International Symposium on Personal, Indoor, and Mobile Radio Communications Conference, Cannes, France, September 2008, and in part at the 2007 International Conference on Signal Processing and Communication Systems, Gold Coast, Australia, December 2007. The review of this paper was coordinated by Dr. J. Li.

The authors are with the College of Engineering and Computer Science, The Australian National University, Canberra, ACT 0200, Australia (e-mail: xiangyun.zhou@anu.edu.au; salman.durrani@anu.edu.au; haley.jones@anu.edu.au).

Color versions of one or more of the figures in this paper are available online at <http://ieeexplore.ieee.org>.

Digital Object Identifier 10.1109/TVT.2009.2026049

same power. Recently, there has been growing interest in using beamforming to improve the connectivity of wireless ad hoc networks [2]–[5]. Beamforming allows the formation of a narrow antenna beam that can be steered to focus most of the signal energy toward a desired direction. In this paper, we provide an analytical model for characterizing the impact of beamforming on the connectivity of wireless ad hoc networks.

For omnidirectional antennas, previous work has analyzed the connectivity of wireless ad hoc networks using different methods and connectivity metrics [6]–[15]. A widely used approach in this regard is the geometric disk model [6], [7]. It is assumed that two nodes can communicate with each other if their distance apart is smaller than a given transmission radius. Using the geometric disk model, a semi-analytical procedure for the determination of the critical node density for an almost surely connected network for the case of simple path loss channels was considered in [9]. The results were extended to a shadowing environment in [10], and it was shown that the channel randomness caused by shadowing can improve network connectivity by reducing the number of isolated nodes. In [11], a probability density function (pdf) of the distance between two nodes in a rectangular or hexagonal region was analytically derived using a space decomposition method and was used to calculate the average number of neighbors of a node (i.e., node degree) with a simple path loss model. The results were extended for the case of multihop networks in a shadowing environment in [12]. An alternative analytical method, which is based on the concept of effective coverage area, was proposed in [13] to analyze the effect of path loss and shadowing on the connectivity of wireless ad hoc networks. It must be noted that the shadowing channel model used in [10], [12], and [13] increases the average channel gain, whereas in a practical wireless channel, shadowing affects only the randomness and not the average value of the channel gain.

More recently, the connectivity of wireless ad hoc networks with different beamforming schemes has been studied in [16]–[22]. Although the size, cost, and power consumption issues limit the applicability of large antenna arrays for wireless mobile devices, the advent of low-cost digital signal processor chips have made beamforming systems practical for commercial use [23], [24] and beamforming is being widely considered for wireless network standards such as IEEE 802.11, IEEE 802.16, and IEEE 802.15.3c [4]. A survey of different beamforming strategies for ad hoc networks was provided in [16]. It is well known that the use of beamforming can improve the network connectivity if each node has knowledge about the locations of all the neighboring nodes. However, the discovery of neighboring nodes in a decentralized network requires

significant signal processing for direction-of-arrival estimation in the implementation of beamforming algorithms [17]. A very simple solution that does not require neighbor node positioning information is the random beamforming strategy [17]. A core idea in random beamforming is that each node in the network randomly selects a main beam direction without any coordination with other nodes. Therefore, the random beamforming scheme has minimal communication overhead and hardware complexity. Using simulations, it was shown that, while random beamforming may decrease the number of neighbors of a node, it leads to an overall improvement in the network connectivity [17]. A similar conclusion, based on simulation studies, was drawn in [19], where the performance of random beamforming is compared to center-directed beamforming, in which each node in the network points its main beam toward the geographic center of the network. A major limitation of the work in [16]–[19] is that it only relies on simulations and provides no analytical solutions. In [20], an analytical study was used to show that random beamforming can both increase and decrease the number of isolated nodes and network connectivity, but no insight was given into when (i.e., under what channel conditions) this occurs. The aforementioned limitations are addressed in this paper.

A. Approach and Contribution

We present an analytical method to characterize the performance of beamforming in the presence of both path loss and shadowing. We extend the work in [13] for ad hoc networks with omnidirectional antennas to include the effects of beamforming. We investigate both the local and the overall connectivity with beamforming: 1) connectivity from the viewpoint of a single node (probability of node isolation) and 2) connectivity from the viewpoint of the entire network (1-connectivity and path probability).

Our initial work in [21] considered the local connectivity performance with random beamforming in simple path loss channels, which was extended to 1-connectivity performance in [22]. Our contribution and innovation in this paper differ from [13] and our previous research in [21] and [22] in three major respects. First, we propose a realistic unbiased shadowing channel model that removes the bias in the average received power due to the lognormal spread of the shadowing. Using the unbiased shadowing channel model, the effect of shadowing on the network connectivity is fundamentally different from the existing results in the literature. Second, we consider both the exact and a simplified beam pattern model in the analysis of random beamforming and extend our analytical approach to include the case of center-directed beamforming. Third, in addition to new analytical results, we include simulation results for path probability, which is a relatively moderate metric for the overall network connectivity compared with 1-connectivity. We show that the impact of shadowing or beamforming on path probability can be different from that on 1-connectivity. The analytical and simulation results in this paper provide fundamental insights into how the channel and beamforming conditions affect the connectivity properties of wireless ad hoc networks.

The following is a summary of the main results in this paper.

- 1) We present a simple intuitive method to calculate the effective coverage area of a node, taking beamforming and a channel model incorporating path loss and unbiased shadowing into account.
- 2) For a fixed path loss exponent α , we prove that the presence of shadowing always reduces the effective coverage area of a node, thereby increasing the probability of node isolation and reducing the network 1-connectivity. This interesting result, which is the opposite of the conclusions in [10], [13], and [22], is because of the realistic unbiased shadowing channel model employed in this paper. In addition, we prove that the detrimental effect of shadowing reaches its maximum at $\alpha = 4$.
- 3) We show that moderate shadowing can improve the path probability between two nodes, while it always reduces the network 1-connectivity. This improvement in the path probability is due to the randomness introduced in the communication range of a node.
- 4) We show that the impact of beamforming strongly depends on the level of the channel path loss. In particular, beamforming improves the connectivity, compared with the use of omnidirectional antennas, for a path loss exponent of $\alpha < 3$.
- 5) Comparing random beamforming and center-directed beamforming, we find that both schemes give similar performance for the local and the overall network connectivity, with center-directed beamforming slightly outperforming random beamforming.

The rest of this paper is organized as follows. In Section II, we present the antenna and channel model. In Section III, we derive the effective coverage area of a node and analytically study the impact of shadowing. Section IV studies the impact of both random beamforming and center-directed beamforming on the effective coverage area. In Section V, we use the effective coverage area results to characterize the connectivity of wireless ad hoc networks. In Section VI, we validate the proposed model by comparing with simulation results and investigate the local and the overall network connectivity. Finally, conclusions are drawn in Section VII.

II. SYSTEM MODEL DESCRIPTION

Consider a wireless ad hoc network, as shown in Fig. 1. The nodes with beamforming antennas are assumed to be randomly distributed in a 2-D space according to a Poisson point process. A homogeneous Poisson process provides an accurate model for a uniform distribution of nodes as the network area approaches infinity [25]. Let ρ denote the node density in nodes per square meter. The probability mass function of the number of nodes X in an area A is given by $P(X = x) = (\mu^x/x!)e^{-\mu}$, where the Poisson distribution parameter $\mu = \rho A$ is the expected number of nodes in the area A .

A. Antenna Model

We assume that all nodes are equipped with identical beamforming array antennas for transmission and reception. The

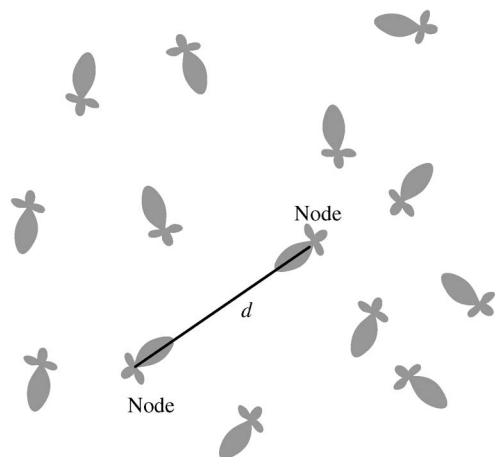


Fig. 1. Wireless ad hoc network with nodes equipped with beamforming antennas, where the beams are pointed in random directions. The two indicated nodes are a distance d apart.

antennas are lossless and devoid of any mutual coupling. In general, the antenna gain is given by [26]

$$G = \frac{|E(\theta, \phi)|^2}{\frac{1}{4\pi} \int_0^{2\pi} \int_0^\pi |E(\theta, \phi)|^2 \sin(\theta) d\theta d\phi} \quad (1)$$

where $\phi \in [0, 2\pi)$ is the angle from the x -axis in the xy plane, $\theta \in [0, \pi)$ is the angle from the z -axis, and $E(\theta, \phi)$ is the electric field strength of the antenna array.

We consider that a uniform-circular-array (UCA) configuration is employed at each node. A UCA configuration is chosen because a circular array has a single main lobe, and the beamwidth of the main lobe is almost independent of the main beam direction [27]. By comparison, a uniform linear array has two main lobes due to symmetry, and the beamwidth significantly varies with the main beam direction [27]. This can lead to an increase in the interference level and an ambiguity in the direction of the incoming signal at a receiver [28]. In addition, UCAs are known to outperform uniform rectangular arrays [29]. It should be noted that our analytical results on beamforming in Section IV and connectivity in Section V are general and apply to any antenna array configuration.

For a UCA of M identical antenna elements, the electric field strength is given by [27]

$$E(\theta, \phi) = \sum_{m=1}^M E_0 \gamma_m \exp[jka \sin(\theta) \cos(\phi - \phi_m)] \quad (2)$$

where E_0 is the electric field pattern of the constituent omnidirectional antennas, which is set to 1 without loss of generality, a is the radius of the circular array, $k = 2\pi/\lambda$ is the wave number, λ is the wavelength of the propagating signal, $\phi_m = 2\pi m/M$ is the angular position of the m th element, and γ_m is the complex excitation for each antenna element. Since the nodes are located on the 2-D xy plane, we consider all beamforming directions to be on the xy plane as well. For classical 2-D beamforming, γ_m is given by [27]

$$\gamma_m = \exp[-jka \sin(\theta_0) \cos(\phi_0 - \phi_m)] \quad (3)$$

where $\theta_0 = \pi/2$ (i.e., the xy plane), and ϕ_0 is the azimuth angle of the desired main beam.

Substituting (3) into (2) and (2) into (1), we can calculate the antenna gain for any azimuthal angle ϕ . Note that the resulting antenna gain G from (1) is a function of ϕ , ϕ_0 , and M . Thus, we denote it as $G(\phi, \phi_0, M)$. In the remainder of this paper, we will use the antenna gain $G(\phi, \phi_0, M)$ to evaluate the impact of beamforming on the network connectivity.

B. Channel Model

We assume that the channel gain between a transmitting and receiving node pair is affected by path loss attenuation and shadowing effects. The severity of the path loss is characterized by the path loss exponent α , which usually ranges from 2 to 5 [30]. The shadowing S is modeled as a random variable drawn from a log-normal distribution given by

$$S = 10^{w/10} \quad (4)$$

where w is a Gaussian random variable with zero mean and standard deviation σ (hence, S is normal in decibels) [31]. A typical value of σ ranges from 4 to 13 dB [32]. Note that both path loss and shadowing are multiplicative factors of the received signal power.

Let P_T denote the transmit power of each node. With path loss and shadowing, the received signal power P_R is given by

$$P_R = \zeta \frac{1}{d^\alpha} C G_T G_R P_T \quad (5)$$

where d is the distance between the transmitting and receiving nodes, $C = (\lambda/(4\pi))^2$ is a constant, G_T and G_R are the antenna gains of the transmitting and receiving nodes, respectively, $\zeta = S/E[S]$ is the normalized shadowing variable, and $E[\cdot]$ denotes statistical expectation.

It is important to note that, unlike the signal models in [10], [12], [13], and [22], we normalize the shadowing term S by its mean value $E[S]$ in the shadowing variable ζ . In practical scenarios, shadowing is caused by the variation of local propagation conditions at different locations. The presence of shadowing introduces a variation in the received signal strength, but it does not change the average value determined by the path loss model [30]. The proposed normalization in ζ removes the bias in the received signal power so that the average received power does not artificially increase with the lognormal spread of the shadowing. The consequences of this normalization will be discussed in the next section.

III. EFFECTIVE COVERAGE AREA ANALYSIS

In this section, we derive the effective coverage area of a node, taking into account beamforming, path loss, and shadowing. Without loss of generality, we can normalize (5) with respect to the constant C so that the power attenuation is expressed as

$$\beta(d) = \frac{P_T}{P_R} = \frac{1}{\zeta} \frac{d^\alpha}{G_T G_R} \quad (6)$$

Assuming identical node hardware and negligible internode interference, two nodes separated by a distance d are connected if $\beta(d) < \beta_{\text{th}}$, where β_{th} is the threshold signal power attenuation. From (6), the probability of having no direct connection between two nodes separated by a distance d is given by

$$\begin{aligned} P(\beta \geq \beta_{\text{th}}) &= P\left(\frac{1}{\zeta} \frac{d^\alpha}{G_T G_R} \geq \beta_{\text{th}}\right) \\ &= P\left((\beta_{\text{th}} \zeta G_T G_R)^{\frac{1}{\alpha}} \leq d\right). \end{aligned} \quad (7)$$

For simplicity, we define the random variable R as

$$R = (\beta_{\text{th}} \zeta G_T G_R)^{\frac{1}{\alpha}}. \quad (8)$$

Substituting (8) into (7), we get $P(\beta \geq \beta_{\text{th}}) = P(R \leq d)$. Hence, the random variable R can be referred to as the *communication range*. That is, the node is able to communicate with all nodes lying within a distance R . The coverage area of a node can thus be considered as a disk with radius R centered at the node. Since R is a random variable, the *effective coverage area* is defined as the expected value of the coverage area given by $E[\pi R^2] = \pi E[R^2]$, where $E[R^2]$ is the second moment of the communication range. As shown in [13], the effective coverage area is strongly related to the connectivity properties of the network. Hence, we now study the impact of shadowing and beamforming on the effective coverage area $E[\pi R^2]$.

We assume that the nodes choose the beamforming strategy independently of the shadowing effects at their locations. From (8), we have

$$\begin{aligned} E[\pi R^2] &= \pi E\left[(\beta_{\text{th}} \zeta G_T G_R)^{\frac{2}{\alpha}}\right] \\ &= \pi (\beta_{\text{th}})^{2/\alpha} E[\zeta^{2/\alpha}] E[(G_T G_R)^{2/\alpha}]. \end{aligned} \quad (9)$$

From (9), we can see that the effects of the shadowing and beamforming on the effective coverage area are characterized by the shadowing factor $E[\zeta^{2/\alpha}]$ and the beamforming factor $E[(G_T G_R)^{2/\alpha}]$, respectively. In the following, we present the results of the shadowing factor. The analysis of the beamforming factor will be performed in the next section.

Theorem 1: The effect of shadowing on the effective coverage area of a randomly chosen node is given by

$$E[\zeta^{2/\alpha}] = \exp\left\{\left(\frac{\ln 10}{10} \sigma\right)^2 \left(\frac{2-\alpha}{\alpha^2}\right)\right\}. \quad (10)$$

Proof: See the Appendix.

From (10), we see that the effect of shadowing depends on both the lognormal standard deviation σ and the path loss exponent α . Since $\alpha > 2$ for any practical wireless channel, the exponent in (10) is always negative. Therefore, Theorem 1 implies that shadowing always results in a reduction of the effective coverage area. This result contradicts previous results in [10], [13], and [22], which do not normalize the shadowing factor. It must be noted that if the normalization is not used, then the impact of shadowing on the effective coverage area is given by $E[S^{2/\alpha}] = \exp\{(\sigma \ln 10 / 5\alpha)^2 / 2\}$ (see the Appendix), where the exponent is always positive, and consequently, shadowing

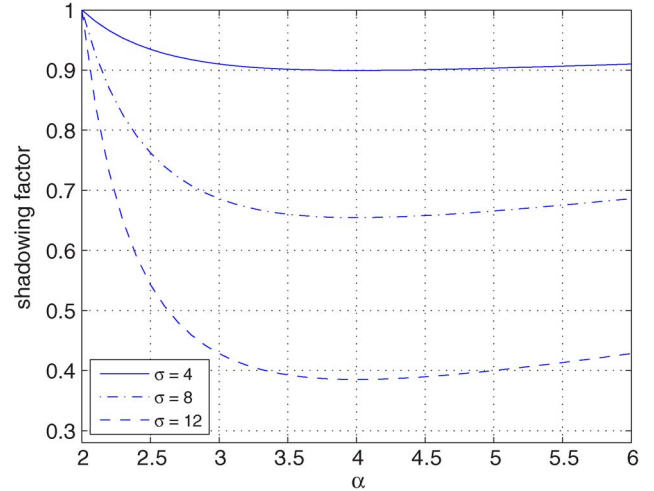


Fig. 2. Shadowing factor in (10) versus path loss exponent α for different values of the shadowing lognormal standard deviation σ (in decibels).

always increases the coverage area, as concluded in [10], [13], and [22].

Furthermore, by examining the first and second derivatives of the shadowing factor $E[\zeta^{2/\alpha}]$ in (10) w.r.t. α , the following corollary can be obtained.

Corollary 1: For any fixed value of σ , the shadowing factor reduces as α increases from 2 to 4, reaching a minimum at $\alpha = 4$, and increases as α increases beyond 4.

Corollary 1 implies that shadowing results in a maximum reduction of the effective coverage area at $\alpha = 4$ for any fixed σ . Similarly, one can fix α and investigate the effect of σ on the shadowing factor. For a fixed α , the first term in the exponent in (10) implies that the shadowing factor decreases as σ increases. Fig. 2 shows the shadowing factor versus α for different values of σ , which confirms the results in Corollary 1. Furthermore, we see from Fig. 2 that the shadowing factor does not change much with α for $\alpha > 3$. On the other hand, the shadowing factor significantly varies with σ for any fixed α .

IV. BEAMFORMING ANALYSIS

In this section, we study the effects of random beamforming and center-directed beamforming on the effective coverage area, which is characterized by the beamforming factor $E[(G_T G_R)^{2/\alpha}]$.

A. Random Beamforming

Random beamforming is a simple scheme that requires no knowledge of the positions of individual nodes or any geographical information about the network. It allows each node in the network to randomly select a main beam direction. Fig. 3(a) shows a pair of transmitting (TX) and receiving (RX) nodes in a random beamforming scenario. The parameters shown in the figure are defined as follows: d = distance between the TX and RX nodes, ϕ = direction of the RX node from the TX node, with respect to the x -axis, ϕ_T = main beam direction of the TX node, and ϕ_R = main beam direction of the RX node.

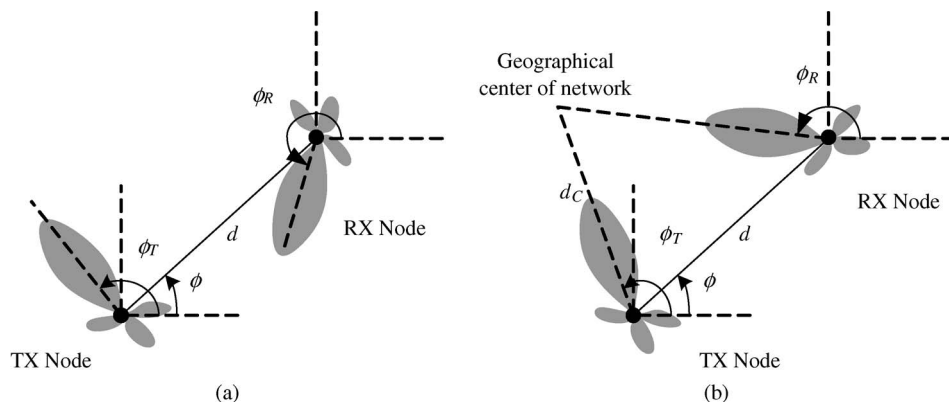


Fig. 3. Relative positions of a transmitting and receiving node pair in (a) random beamforming and (b) center-directed beamforming.

 TABLE I
 BEAMFORMING FACTOR FOR RANDOM BEAMFORMING

Number of antenna elements M	Path loss exponent α													
	2.00	2.25	2.50	2.75	3.00	3.25	3.50	3.75	4.00	4.25	4.50	4.75	5.00	
4	1.48	1.26	1.12	1.02	0.95	0.91	0.87	0.84	0.82	0.80	0.79	0.78	0.77	
6	1.51	1.27	1.12	1.03	0.96	0.92	0.89	0.86	0.85	0.83	0.82	0.82	0.81	
8	1.60	1.31	1.14	1.03	0.96	0.90	0.87	0.84	0.82	0.80	0.79	0.78	0.77	
10	1.84	1.46	1.24	1.10	1.01	0.95	0.90	0.87	0.85	0.83	0.81	0.80	0.79	

For a network utilizing random beamforming, the pdf of the main beam angle has a uniform distribution. Since the nodes are deployed according to a uniform distribution, the direction of any other node from a chosen node has a uniform distribution as well. Therefore, angles ϕ , ϕ_T , and ϕ_R have identical but mutually independent pdf's, being uniformly distributed over $[0, 2\pi)$. Using this argument, the beamforming factor is given by

$$E \left[(G_T G_R)^{\frac{2}{\alpha}} \right] = \frac{1}{(2\pi)^3} \cdot \int_0^{2\pi} \int_0^{2\pi} \int_0^{2\pi} (G(\phi, \phi_T, M) G(\pi + \phi, \phi_R, M))^{\frac{2}{\alpha}} d\phi_R d\phi_T d\phi \quad (11)$$

where $G(\phi, \phi_T, M)$ and $G(\pi + \phi, \phi_R, M)$ are the transmit and receive antenna gains, which can be determined from (1).

In general, a closed-form expression for the beamforming factor in (11) with an exact expression for the antenna gains cannot be obtained. However, it can be seen from (11) that the beamforming factor depends on the path loss exponent α which usually ranges from 2 to 5, and the number of antenna elements M , which is usually less than 10 in practical scenarios. Hence, the form of the aforementioned integral is such that it can quickly and accurately be numerically computed for the values of α and M in the range of interest. Therefore, the computational complexity of studying the beamforming factor using the exact beam pattern is still low.

Using the antenna gain of a UCA given in Section II-A, we numerically evaluate (11), and the results are summarized in Table I for different values of α and M . Note that, for omnidirectional antennas, the beamforming factor is unity. We can see from Table I that the beamforming factor decreases as α increases. However, for a fixed α , the beamforming factor stays relatively constant over a practical range of M (e.g., $M < 10$). For $\alpha < 3$, the beamforming factor is greater than

unity, and beamforming increases the effective coverage area. On the other hand, it decreases the effective coverage area when $\alpha > 3$.

Analysis With a Simplified Beam Pattern Model: A simple beam pattern model was proposed in [33], where the beam pattern consists of a flat main lobe and a flat sidelobe, which is also referred to as the keyhole beam pattern. The parameters associated with the model are the main-lobe width ω (normalized w.r.t. 2π) and the sidelobe attenuation factor ν , with the main-lobe gain being M and the sidelobe gain being νM . Parameters ω and ν are determined based on a given beam pattern by preserving the first- and second-order moments of the beam pattern, i.e., $\omega M + (1 - \omega)\nu M = E[G(\phi, \phi_0, M)]$, and $\omega M^2 + (1 - \omega)(\nu M)^2 = E[G^2(\phi, \phi_0, M)]$. This model was found to be accurate for the capacity and outage probability analysis of beamforming in wireless cellular systems [33], [34].

Using this simplified model, it can be shown that (11), after some manipulations, reduces to a closed-form expression given by

$$E \left[(G_T G_R)^{\frac{2}{\alpha}} \right] = \left(\omega M^{2/\alpha} + (1 - \omega)(\nu M)^{2/\alpha} \right)^2 \quad (12)$$

where

$$\omega = \frac{E[G^2(\phi, \phi_0, M)] - (E[G(\phi, \phi_0, M)])^2}{E[G^2(\phi, \phi_0, M)] - 2E[G(\phi, \phi_0, M)]M + M^2} \quad (13)$$

$$\nu = \frac{1}{M} \frac{E[G^2(\phi, \phi_0, M)] - E[G(\phi, \phi_0, M)]M}{E[G(\phi, \phi_0, M)] - M}. \quad (14)$$

We compute the beamforming factors using the simplified model given in (12) (the results are not shown for brevity). Similar to Table I, we observe that the beamforming factor decreases as α increases. However, the actual values calculated using (12) are usually different from those in Table I. The reason for this difference is that the simplified model only matches the first and second moments of $G(\phi, \phi_0, M)$, while

TABLE II
BEAMFORMING FACTOR FOR CENTER-DIRECTED BEAMFORMING

Number of antenna elements M	Path loss exponent α													
	2.00	2.25	2.50	2.75	3.00	3.25	3.50	3.75	4.00	4.25	4.50	4.75	5.00	
4	1.49	1.28	1.15	1.06	0.99	0.94	0.91	0.88	0.86	0.84	0.83	0.82	0.81	
6	1.57	1.31	1.15	1.05	0.98	0.93	0.89	0.87	0.85	0.83	0.82	0.81	0.81	
8	1.67	1.38	1.21	1.09	1.01	0.95	0.91	0.88	0.86	0.84	0.82	0.81	0.80	
10	2.46	1.88	1.54	1.33	1.18	1.09	1.02	0.97	0.93	0.90	0.88	0.86	0.85	

the computation of the beamforming factor in (11) requires an accurate match of $G^{2/\alpha}(\phi, \phi_0, M)$, with $2 \leq \alpha \leq 5$. Thus, we can conclude that the simplified beam pattern model proposed in [33] for the capacity and outage analysis of beamforming in cellular networks is not suitable for the connectivity analysis of beamforming in ad hoc networks.

B. Center-Directed Beamforming

The major drawback of random beamforming is the *border effect*. That is, the nodes located at the border of the network may happen to steer their main beams in a direction outside the network area, causing loss of connectivity [17]. If the area of the network is relatively fixed, it is possible for the nodes to be given or learn the geographical information of the network. The cost and complexity of obtaining the information on the center of the network is much lower than that of obtaining the positions of individual nodes. In this scenario, center-directed beamforming can be adopted, where each node points its main beam toward the center of the network.

Fig. 3(b) shows a scenario with center-directed beamforming, where each node directs its main beam toward the geographical center of the network. In Fig. 3(b), d_C denotes the distance of the TX node from the geographical center of the network, and the remaining parameters are defined as in Fig. 3(a).

To simplify the analysis, we make the assumption that the distances between the directly (i.e., one-hop) connected node pairs are much smaller than their distances from the geographical center of the network, such that $d \ll d_C$. This assumption is reasonably accurate in many practical situations where the majority of one-hop connected node pairs are a relatively large distance from the center of the network, compared with the distance between the node pairs themselves. Using this assumption, it can be shown that the one-hop-connected node pairs have approximately the same main beam direction, as they all point their main beams toward the center, such that $\phi_R \approx \phi_T$. By letting $\phi_R = \phi_T$ for all node pairs, we can establish a simplified model to approximate the beamforming factor for the center-directed beamforming scheme.

As previously discussed, for a uniformly distributed network, ϕ and ϕ_T have uniform distributions over $[0, 2\pi)$. Therefore, an approximation of the beamforming factor for center-directed beamforming can be expressed as

$$E \left[(G_T G_R)^{\frac{2}{\alpha}} \right] \approx \frac{1}{(2\pi)^2} \int_0^{2\pi} \int_0^{2\pi} (G(\phi, \phi_T, M) G(\pi + \phi, \phi_T, M))^{\frac{2}{\alpha}} d\phi_T d\phi. \quad (15)$$

We can see that (15) depends on the path loss exponent α and the number of antenna elements M , and it can quickly and accurately be numerically computed for the values of α and M in the range of interest. Therefore, we numerically evaluate (15) and summarize the results in Table II. Similar to random beamforming, we also compute the beamforming factor using the simplified beam pattern model (the results are not shown for brevity)¹ and find that the values are usually different from the ones in Table II, which again indicates that the simplified beam pattern model is not suitable for the connectivity analysis of beamforming in wireless ad hoc networks.

Comparing the results in Tables I and II, we see that the beamforming factors for random beamforming and center-directed beamforming behave very similarly, with the beamforming factors for center-directed beamforming being slightly higher for given values of α and M . Therefore, the effective coverage area of a node is slightly larger in a center-directed beamforming network than that in a random beamforming network.

V. CONNECTIVITY ANALYSIS

In this section, we characterize the connectivity of wireless ad hoc networks with beamforming. We consider both the local network connectivity (probability of node isolation) and the overall network connectivity (1-connectivity and path probability).

A. Local Network Connectivity

The probability of node isolation, which is denoted by $P(\text{iso})$, is defined as the probability that a randomly selected node in an ad hoc network has no connections to any other nodes. It is a measure of the local network connectivity, and its general expression is given by [9]

$$P(\text{iso}) = \exp \{-E[D]\} \quad (16)$$

where D denotes the node degree, which is defined as the number of direct links that any given node has to other nodes. For a node deployment following a homogeneous Poisson point process with density ρ , the node degree has a Poisson distribution with parameter $\rho E[\pi R^2]$ [13]. Therefore, the average node degree $E[D]$ is given by

$$E[D] = \rho E[\pi R^2] = \rho \pi (\beta_{\text{th}})^{2/\alpha} E[\zeta^{2/\alpha}] E \left[(G_T G_R)^{2/\alpha} \right] \quad (17)$$

¹With the simplified beam pattern model given in [33], it can be shown that the beamforming factor in (15) reduces to $E[(G_T G_R)^{2/\alpha}] \approx 2\omega \nu^{2/\alpha} M^{4/\alpha} + (1 - 2\omega)(\nu M)^{4/\alpha}$.

where (9) is used to obtain (17). Substituting (17) into (16), we can determine the probability of isolation with beamforming to be

$$P(\text{iso}) = \exp \left\{ -\rho \pi (\beta_{\text{th}})^{2/\alpha} E[\zeta^{2/\alpha}] E \left[(G_T G_R)^{2/\alpha} \right] \right\} \quad (18)$$

where $E[\zeta^{2/\alpha}]$ is given by (10), and $E[(G_T G_R)^{2/\alpha}]$ is given by (11) or (15).

Remark 1: From Theorem 1 in Section III, we know that the shadowing factor $E[\zeta^{2/\alpha}]$ is always negative for wireless channels with $\alpha > 2$. Therefore, the presence of shadowing always increases the probability of node isolation given in (18). Furthermore, from the values of the beamforming factor $E[(G_T G_R)^{2/\alpha}]$ given in Tables I and II, we conclude that the use of beamforming, compared with omnidirectional antennas, reduces the probability of node isolation when the path loss exponent is lower than 3, and it increases node isolation when the path loss exponent is higher than 3. It must be noted that the reduction in the local connectivity is not always detrimental. For example, the reduction in the node degree may result in a reduction in the interference level if the internode interference needs to be considered.

B. Overall Network Connectivity

1-connectivity, which is denoted by $P(1\text{-con})$, is defined as the probability that every node pair in the network has at least one path connecting them. It is a relatively strong measure of the overall network connectivity. An upper bound for the network 1-connectivity is given by [9]

$$P(1 - \text{con}) < \exp \{ -\rho A P(\text{iso}) \} \quad (19)$$

where A is the area of the network, $P(\text{iso})$ is given in (16), and $\exp \{ -\rho A P(\text{iso}) \}$ is the probability of no isolated nodes in the network. It can be shown from the theorems of geometric random graphs [7] that the bound for 1-connectivity in (19) is tight as the probability approaches unity for a path-loss channel [9]. The tightness of the bound at high connectivity has also been found for shadowing channels [10].

For 1-connectivity analysis, we focus on the node density that yields an almost surely connected network, that is, the density at which $P(1\text{-con}) = 0.99$ [10]. This is referred to as the critical node density, which is denoted by ρ_c . Since the bound in (19) is very tight at $P(1\text{-con}) \approx 1$, we can use it to calculate ρ_c . The critical node density can be solved from (19) using Lambert's W function as

$$\begin{aligned} \rho_c &= -\frac{1}{E[\pi R^2]} W_{-1} \left(\frac{E[\pi R^2] \ln 0.99}{A} \right) \\ &= -\frac{1}{\pi (\beta_{\text{th}})^{2/\alpha} E[\zeta^{2/\alpha}] E \left[(G_T G_R)^{2/\alpha} \right]} \\ &\quad W_{-1} \left(\frac{\ln 0.99}{A} \pi (\beta_{\text{th}})^{2/\alpha} E[\zeta^{2/\alpha}] E \left[(G_T G_R)^{2/\alpha} \right] \right) \quad (20) \end{aligned}$$

where W_{-1} denotes the real-valued nonprincipal branch of Lambert's W function.

Remark 2: With the upper bound on 1-connectivity given in (19), we know that 1-connectivity reduces as the probability of node isolation increases. Since the presence of shadowing and the use of beamforming at a high path loss exponent ($\alpha > 3$) increase node isolation, a higher critical node density ρ_c is required to establish an almost surely connected network in these scenarios. On the other hand, ρ_c can be reduced by using beamforming when the path loss exponent is low ($\alpha < 3$).

Another measure of the overall network connectivity is path probability, which is denoted by $P(\text{path})$ and is defined as the probability that two randomly chosen nodes are connected via either a direct link or a multihop path. It is a relatively moderate metric compared with 1-connectivity. An analytical expression for the path probability is still an open research problem [17]. Therefore, we will carry out simulations in the next section to illustrate the effects of beamforming on path probability. Our analytical approach, however, allows us to make the following intuitive observations regarding the effects of shadowing and beamforming on path probability.

Remark 3: The effects of shadowing and the effects of beamforming, particularly random beamforming, are very similar, as both create randomness in the node communication range. The presence of shadowing introduces randomness in the received signal power for nodes at different locations. On the other hand, a beamforming node loses links to closely located neighbors in some directions, while it creates links to nodes that are farther away in other directions. Furthermore, it has been shown in [17] and [19] that a reduction in the local network connectivity may result in an improvement in the path probability by the use of beamforming, particularly in sparse networks. A beamforming node creates links to nodes that are farther away in certain directions, and it is the long links that improve the path probability. As the effect of shadowing is very similar to that of beamforming, we can expect that the presence of shadowing may improve the path probability, particularly in sparse networks, although it reduces the local network connectivity.

VI. RESULTS

In this section, we present the numerical results of the effect of shadowing and beamforming on the connectivity of wireless ad hoc networks. We verify the analytical models and insights given in Sections III, IV, and V by comparing them with simulations. In the simulations, nodes are randomly distributed according to a uniform distribution on a square of area $B \text{ m}^2$. To eliminate border effects, we use the sub-area simulation method [9], such that we only compute the connectivity measures for nodes located on an inner square of area $A \text{ m}^2$, where A is sufficiently smaller than B . The simulation results are then calculated by averaging over 5000 Monte Carlo simulation trials.

A. Effect of Shadowing

To validate the analytical model for studying the effect of shadowing in Section III, we compare the analytical and simulation results on the probability of node isolation. Fig. 4 shows the probability of node isolation versus node density for $\beta_{\text{th}} = 50 \text{ dB}$, $M = 1$ (omnidirectional antennas), $\alpha = 2.5, 3$, and 4, and $\sigma = 0, 4$, and 8 dB. The analytical results shown using lines

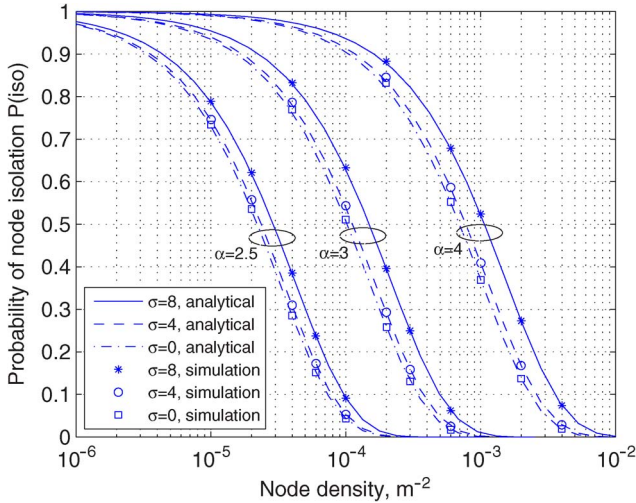


Fig. 4. Probability of node isolation versus node density with $M = 1$ (omnidirectional antennas) and system parameters $\beta_{th} = 50$ dB, $\alpha = 2.5, 3$, and 4 , and $\sigma = 0, 4$, and 8 dB (lines = analytical results from (18) and markers = simulation results).

TABLE III
CRITICAL NODE DENSITY: EFFECT OF SHADOWING

α	β_{th} (dB)	A (m ²)	σ (dB)	M	Analytical results in [10]	Analytical results computed using (20)
3	50	10^5	0	1	1.41×10^{-3}	1.44×10^{-3}
3	50	10^5	4	1	1.14×10^{-3} (-19%)	1.60×10^{-3} (+11%)
3	50	10^5	8	1	6.05×10^{-4} (-57%)	2.19×10^{-3} (+52%)
4	50	10^5	0	1	-	1.19×10^{-2}
4	50	10^5	4	1	1.05×10^{-2}	1.34×10^{-2} (+13%)
4	50	10^5	8	1	-	1.89×10^{-2} (+59%)

are calculated from (18), and the simulation results are indicated by markers. We see that the simulation results are in excellent agreement with the analytical results in all cases. For a fixed α , we see that $P(iso)$ increases as σ increases. That is, shadowing results in more isolated nodes in the network. In addition, we see that the negative effect of shadowing becomes more noticeable as α increases from 2.5 to 4. These trends agree with our earlier observations in Sections III and V-A.²

For 1-connectivity, we focus on the critical node density ρ_c , which ensures an almost connected network, i.e., $P(1-con) = 0.99$. Table III summarizes the values of ρ_c for system parameters $\beta_{th} = 50$ dB, $A = 10^5$ m², and $M = 1$. It also includes the corresponding ρ_c from [10] for comparison. Our results in Table III show that, for any given α , the presence of shadowing increases the critical node density, while the results in [10] show the opposite trend due to the absence of normalization in the shadowing factor. For example, at $\alpha = 3$, we see that the network requires an additional 11% of the total number of nodes to be almost surely connected from a non-shadowing channel to a shadowing channel with $\sigma = 4$ dB. This increases to an additional 52% of the total number nodes required if $\sigma = 8$ dB. We also see that the percentage increase in the critical node density due to shadowing becomes larger when α increases from 3 to 4, which agrees with Corollary 1 in Section III. These results show that the presence of shadowing is detrimental for 1-connectivity.

²We have also verified our analytical results for other values of M and have observed the same trends. The results are not shown for brevity.

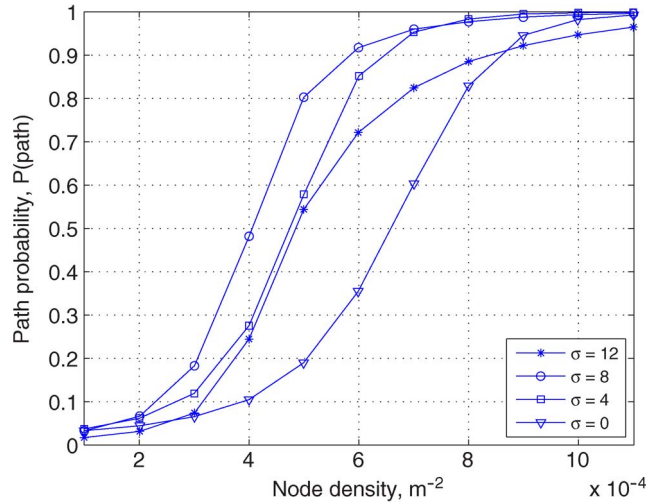


Fig. 5. Path probability versus node density with $M = 1$ (omnidirectional antennas) and system parameters $\beta_{th} = 50$ dB, $\alpha = 3$, and $\sigma = 0, 4, 8$, and 12 dB.

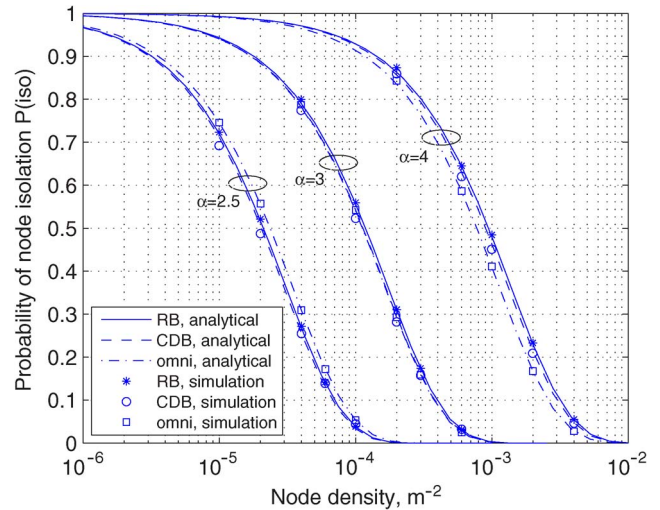


Fig. 6. Probability of node isolation versus node density with $M = 4$ antennas and system parameters $\beta_{th} = 50$ dB, $\alpha = 2.5, 3$, and 4 , and $\sigma = 4$ dB (lines = analytical results from (18), markers = simulation results, RB = random beamforming, and CDB = center-directed beamforming).

As mentioned in Section V-B, an analytical expression for the path probability is still an open research problem; hence, we present simulation results and focus on the overall trends. Fig. 5 shows the path probability versus node density for $M = 1$, $\alpha = 3$, $\beta_{th} = 50$ dB, $A = 2.5 \times 10^5$ m², and different shadowing environments with σ ranging from 0 (no shadowing) to 12 dB. Unlike 1-connectivity, we see that the presence of moderate shadowing, e.g., $\sigma = 4$ or 8 dB, significantly improves $P(path)$. For example, $P(path)$ at $\rho = 6 \times 10^{-4}$ m⁻² for $\sigma = 0$ dB is 0.35, and that for $\sigma = 8$ dB is 0.92. This agrees with our expectation in Section V-B that the presence of shadowing may increase the path probability, although it reduces the local network connectivity. However, $P(path)$ does not always increase with σ . As shadowing becomes severe, e.g., $\sigma = 12$ dB, $P(path)$ is lower than that achieved in a moderate shadowing environment. We confirmed that these trends are also observed at other values of α .

TABLE IV
CRITICAL NODE DENSITY: EFFECT OF BEAMFORMING

Beamforming Scheme	α	β_{th} (dB)	A (m ²)	σ (dB)	M	Analytical results computed using (20)
Omnidirectional	2.5	50	10 ⁶	8	1	4.55 × 10 ⁻⁴
Random		50	10 ⁶	8	4	4.01 × 10 ⁻⁴ (-12%)
Center-directed		50	10 ⁶	8	4	3.90 × 10 ⁻⁴ (-14%)
Omnidirectional	3	50	10 ⁶	8	1	2.72 × 10 ⁻³
Random		50	10 ⁶	8	4	2.88 × 10 ⁻³ (+6%)
Center-directed		50	10 ⁶	8	4	2.75 × 10 ⁻³ (+1%)
Omnidirectional	4	50	10 ⁶	8	1	2.26 × 10 ⁻²
Random		50	10 ⁶	8	4	2.80 × 10 ⁻² (+24%)
Center-directed		50	10 ⁶	8	4	2.66 × 10 ⁻² (+18%)

B. Effect of Beamforming

Fig. 6 shows the probability of node isolation versus node density for $\beta_{th} = 50$ dB, $\alpha = 2.5, 3$, and 4 , $\sigma = 4$ dB, and $M = 4$ antennas. The analytical results for random and center-directed beamforming are shown in solid lines and dashed lines, respectively. The analytical results for omnidirectional antennas are shown in dash-dotted lines for reference. The simulation results for random beamforming are again in excellent agreement with the analytical results in all cases, which validates the analytical model for random beamforming presented in Section IV-A. For center-directed beamforming, the simulation results are accurate for $\alpha = 4$. Although the accuracy slightly reduces as α decreases from 4 to 3 and 2.5,³ the analytical model presented in Section IV-B provides a reasonably good approximation. From Fig. 6, we see that the use of beamforming results in a lower $P(iso)$ when $\alpha < 3$ and a higher $P(iso)$ when $\alpha > 3$. This agrees with our analytical results for the beamforming factor in Sections IV and V-A.⁴

Table IV illustrates the effect of beamforming on the critical node density ρ_c for system parameters $\beta_{th} = 50$ dB, $A = 10^6$ m², and $\sigma = 8$. We see that the use of beamforming decreases ρ_c at $\alpha = 2.5$, while it increases ρ_c at $\alpha = 3$ and 4 . This implies that beamforming improves 1-connectivity at small path loss exponents and reduces 1-connectivity at large path loss exponents. We also see that center-directed beamforming slightly outperforms random beamforming in all cases. These trends agree with the analytical results in Sections IV-A and IV-B.

Next, we present the simulation results for path probability. We focus on the general trends of the effect of random and center-directed beamforming. Fig. 7 shows the path probability versus node density with $M = 4$ in a moderate shadowing environment, where $\sigma = 8$ dB for networks utilizing random beamforming, center-directed beamforming, and omnidirectional antennas. As the impact of beamforming strongly depends on the path loss exponent α , we include $P(path)$ for both $\alpha = 3$ and $\alpha = 4$. Note that the threshold power attenuation β_{th} is chosen to be different in the two scenarios so that all results can clearly be shown in one figure. By doing so,

³As α reduces, the distances between the directly connected node pairs increases. Therefore, the assumption of $d \ll d_C$ in the model for center-directed beamforming becomes less accurate, which results in the slight mismatch between the analytical and simulation results.

⁴We have also verified our analytical results for other values of σ and have observed the same trends. The results are not shown for brevity.

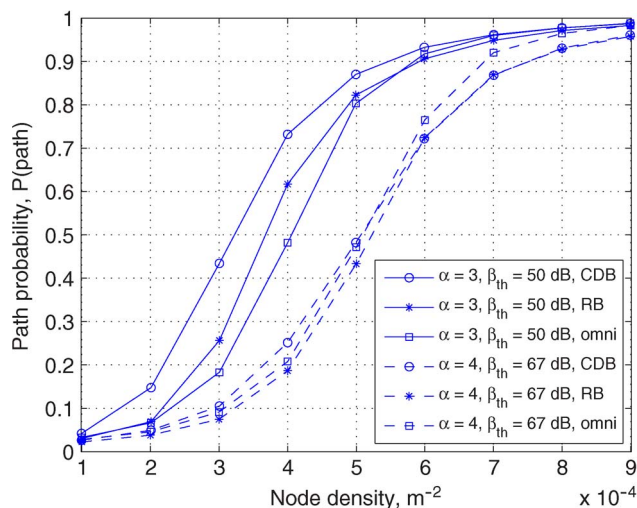


Fig. 7. Path probability versus node density with $M = 4$ antennas and system parameters $\beta_{th} = 50, 67$ dB, $\alpha = 3$ and 4 , and $\sigma = 8$ dB (RB = random beamforming and CDB = center-directed beamforming).

one can easily compare the connectivity improvement from beamforming for different values of α . However, one cannot directly compare the value of $P(path)$ for $\alpha = 3$ with that for $\alpha = 4$. We see from Fig. 7 that the use of beamforming provides a certain improvement in $P(path)$ at $\alpha = 3$ for a relatively low node density, i.e., sparse networks. Moreover, we see that center-directed beamforming generally outperforms random beamforming. For example, $P(path)$ at $\rho = 4 \times 10^{-4}$ m⁻² is 0.62 for random beamforming and 0.73 for center-directed beamforming. These trends are different from those observed in the non-shadowing environment in [19], where it was found that random beamforming usually outperforms center-directed beamforming. In addition, we see that the improvement in $P(path)$ by either beamforming technique is negligible at $\alpha = 4$. Since the beamforming factor decreases with α , we can expect that there is little improvement or even a reduction in path probability by using beamforming when $\alpha > 4$.

C. Effect of Non-Uniform Distribution

In this paper, we have considered a uniform distribution of nodes in the network. It can be argued that this assumption is more accurate in the initial stage after the nodes have uniformly been deployed at random. Due to node mobility, the spatial distribution may gradually become non-uniform, with the nodes tending to form clusters in the network [35]. The analysis for

TABLE V
SUMMARY OF RESULTS

Connectivity Metric	Analytical Expression	Impact of Shadowing	Impact of Beamforming
Probability of Node Isolation	(18)	Detrimental	Beneficial when $\alpha < 3$ Detrimental when $\alpha > 3$
Critical Node Density for 1-connectivity	(20)	Detrimental	Beneficial when $\alpha < 3$ Detrimental when $\alpha > 3$
Path Probability	-	Beneficial at moderate shadowing <i>e.g.</i> , $\sigma = 4, 8$	Beneficial in sparse networks at low to moderate path loss exponent <i>e.g.</i> , $\alpha < 4$

the case of non-uniform distribution is outside the scope of this paper. However, using the insights provided in this paper, we can make the following observation regarding the effect of non-uniform distribution. Since beamforming increases the maximum communication range, it can assist nodes in different clusters to communicate with each other, i.e., build bridges between the clusters. Therefore, we expect that beamforming performs better in a non-uniformly distributed network than in a uniformly distributed network. The results of the effect of beamforming presented in this paper can then be seen as worst-case scenario results.

VII. CONCLUSION

In this paper, we have proposed an analytical model to investigate the effects of shadowing and beamforming on the connectivity of wireless ad hoc networks. Both random and center-directed beamforming schemes for nodes equipped with multiple antennas have been considered. We have derived the effective coverage area of a node, taking into account path loss, shadowing, and beamforming. A shadowing factor and a beamforming factor have been defined to characterize the effects of shadowing and beamforming on the local and the overall connectivity of the network. The accuracy of our analytical model has been verified by comparison with simulation results. Table V summarizes the important findings in this paper.

APPENDIX PROOF OF THEOREM 1

To prove Theorem 1, we need to use the following result given in [25].

Lemma 1: If a random variable $Z = \ln Y$ has a normal distribution with mean and standard deviation given by μ_Z and σ_Z , the mean of Y is given by $E[Y] = \exp\{\mu_Z + (\sigma_Z^2/2)\}$.

Taking the natural logarithm of S in (4), we get

$$\ln S = \ln(10^{w/10}) = \frac{w}{10} \ln 10 = \left(\frac{\ln 10}{10}\right) w \quad (21)$$

where w is a Gaussian random variable with zero mean and standard deviation σ . Therefore, using Lemma 1, the expected value of S is given by

$$E[S] = \exp\left\{\frac{\left(\frac{\ln 10}{10}\sigma\right)^2}{2}\right\}. \quad (22)$$

Similarly, the expected value of $S^{2/\alpha}$ is given by

$$E[S^{2/\alpha}] = E[10^{w/5\alpha}] = \exp\left\{\frac{\left(\frac{\sigma \ln 10}{5\alpha}\right)^2}{2}\right\}. \quad (23)$$

From (22) and (23), the impact of shadowing on the effective coverage area is given by

$$\begin{aligned} E[\zeta^{2/\alpha}] &= \frac{E[S^{2/\alpha}]}{(E[S])^{2/\alpha}} = \frac{\exp\left\{\frac{\left(\frac{\sigma \ln 10}{5\alpha}\right)^2}{2}\right\}}{\exp\left\{\frac{\left(\frac{\ln 10}{10}\sigma\right)^2}{\alpha}\right\}} \\ &= \exp\left\{\left(\frac{\ln 10}{10}\sigma\right)^2 \left(\frac{2}{\alpha^2} - \frac{1}{\alpha}\right)\right\} \\ &= \exp\left\{\left(\frac{\ln 10}{10}\sigma\right)^2 \left(\frac{2-\alpha}{\alpha^2}\right)\right\}. \end{aligned} \quad (24)$$

ACKNOWLEDGMENT

The authors would like to thank the anonymous reviewers for their valuable comments.

REFERENCES

- [1] O. K. Tonguz and G. Ferrari, *Ad Hoc Wireless Networks*. Hoboken, NJ: Wiley, 2006.
- [2] J. H. Winters, "Smart antenna techniques and their application to wireless ad hoc networks," *IEEE Wireless Commun.*, vol. 13, no. 4, pp. 77–83, Aug. 2006.
- [3] C. Sun, J. Cheng, and T. Ohira, Eds., *Handbook on Advancements in Smart Antenna Technologies for Wireless Networks*. Hershey, PA: Inf. Sci. Ref., Jul. 2008.
- [4] P.-C. Yeh, W. E. Stark, and S. A. Zummo, "Performance analysis of wireless networks with directional antennas," *IEEE Trans. Veh. Technol.*, vol. 57, no. 5, pp. 3187–3199, Sep. 2008.
- [5] B. Chen and M. J. Gans, "MIMO communications in ad hoc networks," *IEEE Trans. Signal Process.*, vol. 54, no. 7, pp. 2773–2783, Jul. 2006.
- [6] E. N. Gilbert, "Random plane networks," *SIAM J.*, vol. 9, pp. 533–543, 1961.
- [7] M. D. Penrose, "On k-connectivity for a geometric random graph," *Random Struct. Algorithms*, vol. 15, no. 2, pp. 145–164, 1999.
- [8] L. Booth, J. Bruck, M. Cook, and M. Franceschetti, "Ad hoc wireless networks with noisy links," in *Proc. IEEE ISIT*, Yokohama, Japan, Jun. 2003, p. 386.
- [9] C. Bettstetter, "On the connectivity of ad hoc networks," *Comput. J.*, vol. 47, no. 4, pp. 432–447, Jul. 2004.
- [10] C. Bettstetter and C. Hartmann, "Connectivity of wireless multihop networks in a shadow fading environment," *Wirel. Netw.*, vol. 11, no. 5, pp. 571–579, Sep. 2005.
- [11] P. Fan, G. Li, K. Cai, and K. B. Letaief, "On the geometrical characteristic of wireless ad-hoc networks and its application in network performance analysis," *IEEE Trans. Wireless Commun.*, vol. 6, no. 4, pp. 1256–1264, Apr. 2007.

- [12] S. Mukherjee and D. Avidor, "Connectivity and transmit-energy considerations between any pair of nodes in a wireless ad hoc network subject to fading," *IEEE Trans. Veh. Technol.*, vol. 57, no. 2, pp. 1226–1242, Mar. 2008.
- [13] D. Miorandi, E. Altman, and G. Alfano, "The impact of channel randomness on coverage and connectivity of ad hoc and sensor networks," *IEEE Trans. Wireless Commun.*, vol. 7, no. 3, pp. 1062–1072, Mar. 2008.
- [14] J. Kazemitabar, H. Yousefi'zadeh, and H. Jafarkhani, "The impacts of physical layer parameters on the connectivity of ad-hoc networks," in *Proc. IEEE ICC*, Istanbul, Turkey, Jun. 2006, pp. 1891–1896.
- [15] H. Yousefi'zadeh, H. Jafarkhani, and J. Kazemitabar, "A study of connectivity in MIMO fading ad hoc networks," *J. Commun. Netw.*, vol. 11, no. 1, pp. 47–56, 2009.
- [16] R. Vilzmann, J. Widmer, I. Aad, and C. Hartmann, "Low-complexity beamforming techniques for wireless multihop networks," in *Proc. IEEE Conf. SECON*, Reston, VA, 2006, pp. 489–497.
- [17] C. Bettstetter, C. Hartmann, and C. Moser, "How does randomized beamforming improve the connectivity of ad hoc networks?" in *Proc. IEEE ICC*, Seoul, Korea, May 2005, vol. 5, pp. 3380–3385.
- [18] R. Vilzmann, C. Bettstetter, and C. Hartmann, "On the impact of beamforming on interference in wireless mesh networks," in *Proc. IEEE Workshop WiMesh*, Santa Clara, CA, Sep. 2005, pp. 127–133.
- [19] X. Zhou, H. M. Jones, S. Durrani, and A. Scott, "Effect of beamforming on the connectivity of ad hoc networks," in *Proc. AusCTW*, Adelaide, Australia, Feb. 2007, pp. 13–18.
- [20] H. Koskinen, "Analytical study of connectivity in wireless multihop networks utilizing beamforming," in *Proc. ACM/IEEE Int. Symp. MSWiM*, Torremolinos, Spain, Oct. 2006, pp. 212–218.
- [21] X. Zhou, S. Durrani, and H. M. Jones, "Analytical study of connectivity in wireless ad hoc networks with random beamforming," in *Proc. ICSPCS*, Gold Coast, Australia, Dec. 2007, pp. 321–325.
- [22] S. Durrani, X. Zhou, and H. M. Jones, "Connectivity of wireless ad hoc networks with random beamforming: An analytical approach," in *Proc. IEEE Int. Symp. PIMRC*, Cannes, France, Sep. 2008, pp. 1–5.
- [23] T. Kaiser, "When will smart antennas be ready for the market? Part I," *IEEE Signal Process. Mag.*, vol. 22, no. 2, pp. 87–92, Mar. 2005.
- [24] A. Hottinen, M. Kuusela, K. Hugl, J. Zhang, and B. Raghathan, "Industrial embrace of smart antennas and MIMO," *IEEE Wireless Commun.*, vol. 13, no. 4, pp. 8–16, Aug. 2006.
- [25] D. D. Wackerly, W. Mendenhall, and R. L. Scheaffer, *Mathematical Statistics With Applications*. Belmont, CA: Duxbury, 2002.
- [26] J. D. Kraus, *Antennas*. New York: McGraw-Hill, 1950.
- [27] C. A. Balanis, *Antenna Theory*. Hoboken, NJ: Wiley, 2005.
- [28] A. Munari, F. Rossetto, and M. Zorzi, "A new cooperative strategy for deafness prevention in directional ad hoc networks," in *Proc. IEEE ICC*, Glasgow, U.K., Jun. 2007, pp. 3154–3160.
- [29] P. Ioannides and C. A. Balanis, "Uniform circular and rectangular arrays for adaptive beamforming applications," *IEEE Antennas Wireless Propag. Lett.*, vol. 4, pp. 351–354, 2005.
- [30] T. S. Rappaport, *Wireless Communications: Principles and Practice*. Englewood Cliffs, NJ: Prentice-Hall, 2002.
- [31] M. Schwartz, *Mobile Wireless Communications*. Cambridge, U.K.: Cambridge Univ. Press, 2005.
- [32] A. J. Goldsmith, *Wireless Communications*. Cambridge, U.K.: Cambridge Univ. Press, 2005.
- [33] J. Yu, Y. D. Yao, A. Molisch, and J. Zhang, "Performance evaluation of CDMA reverse links with imperfect beamforming in a multicell environment using a simplified beamforming model," *IEEE Trans. Veh. Technol.*, vol. 55, no. 3, pp. 1019–1031, May 2006.

- [34] H. Li, Y. D. Yao, and J. Yu, "Outage probabilities of wireless systems with imperfect beamforming," *IEEE Trans. Veh. Technol.*, vol. 55, no. 5, pp. 1503–1515, Sep. 2006.
- [35] M. Gyarmati, U. Schilcher, G. Brandner, C. Bettstetter, Y. W. Chung, and Y. H. Kim, "Impact of random mobility on the inhomogeneity of spatial distributions," in *Proc. IEEE Globecom*, New Orleans, LO, Nov. 2008, pp. 1–5.



Xiangyun Zhou (S'08) received the B.E.(Hons.) degree in electronics and telecommunications engineering in 2007 from The Australian National University, Canberra, ACT, Australia, where he is currently working toward the Ph.D. degree in engineering and information technology with the Research School of Information Sciences and Engineering, College of Engineering and Computer Science.

His research interests are in signal processing for wireless communications, including multiple-input–multiple-output systems, ad hoc networks, and relay and cooperative networks.



Salman Durrani (S'00–M'05) received the B.Sc. (first-class honors) degree in electrical engineering from the University of Engineering and Technology, Lahore, Pakistan, in 2000 and the Ph.D. degree in electrical engineering from the University of Queensland, Brisbane, Australia, in December 2004.

Since March 2005, he has been a Lecturer with the College of Engineering and Computer Science, The Australian National University, Canberra, ACT, Australia. He has 32 publications to date in refereed international journals and conferences.

His current research interests include wireless and mobile networks, connectivity of sensor/ad-hoc networks and vehicular networks, channel estimation, and multiple-input–multiple-output and smart antenna systems.

Dr. Durrani is a Member of the Institution of Engineers, Australia. He was the recipient of a University Gold Medal during his undergraduate studies and an International Postgraduate Research Scholarship, which was funded by the Australian government, for the duration of his Ph.D. studies.



Haley M. Jones received the B.E.(Hons.) degree in electrical and electronic engineering and the B.Sc. degree from the University of Adelaide, Adelaide, SA, Australia, in 1992 and 1995, respectively, and the Ph.D. degree in telecommunications engineering from The Australian National University, Canberra, ACT, Australia, in October 2002.

She has been with the College of Engineering and Computer Science, The Australian National University, since January 2002. Her previous experience includes time in industry and working on speech coding with the Cooperative Research Centre for Robust and Adaptive Systems, Canberra, Australia, from 1993 to 1999. Her research interests have included wireless channel modeling, beamforming, and channel and topology issues in mobile ad hoc networks. She has recently branched out into sustainable systems with a particular emphasis on the cradle-to-cradle paradigm.